Met. Mater. Int., Vol. 22, No. 2 (2016), pp. 204~208
doi: 10.1007/s12540-016-5130-x

Effect of Yttrium on Martensite-Austenite Phase Transformation Temperatures and High Temperature Oxidation Kinetics of Ti-Ni-Hf High-Temperature Shape Memory Alloys

Jeoung Han Kim[1,*], Kyong Min Kim[2], Jong Taek Yeom[2,*], and Sung Young[3]

[1]Department of Advanced Materials Engineering, Hanbat National University, Daejeon 34158, South Korea
[2]Titanium Department, Korea Institute of Materials Science, Changwon 51508, South Korea
[3]School of Mechanical Engineering, Korea University of Technology and Education, Chonan 31253, South Korea

(received date: 11 March 2015 / accepted date: 30 November 2015)

The effect of yttrium (< 5.5 at%) on the martensite-austenite phase transformation temperatures, microstructural evolution, and hot workability of Ti-Ni-Hf high-temperature shape memory alloys is investigated. For these purposes, differential scanning calorimetry, hot compression, and thermo-gravimetric tests are conducted. The phase transformation temperatures are not noticeably influenced by the addition of yttrium up to 4.5 at%. Furthermore, the hot workability is not significantly affected by the yttrium addition up to 1.0 at%. However, when the amount of yttrium addition exceeds 1.0 at%, the hot workability deteriorates significantly. In contrast, remarkable improvement in the high temperature oxidation resistance due to the yttrium addition is demonstrated. The total thickness of the oxide layers is substantially thinner in the Y-added specimen. In particular, the thickness of (Ti,Hf) oxide layer is reduced from ~200 μm to ~120 μm by the addition of 0.3 at% Y.

Keywords: shape memory alloy, precipitation, phase transformation temperature, oxidation, yttrium

1. INTRODUCTION

Ti-Ni-Hf is a high-temperature shape memory alloy that can be used in actuator applications in mobile phones, automobiles, rocket engines, and other devices [1-3]. In order to use the material as a micro-actuator in mobile phones, it must be fabricated in the form of a thin wire with a diameter of less than 0.1 mm or a thin sheet with thickness less than 0.1 mm in order to demonstrate a fast response. In general, due to its extremely poor ductility, hot working at 800-1000 °C is inevitable in the fabrication process of this type of material. However, even high temperature forging or forming is not always successful [4]. Several reasons for this poor hot workability have been proposed: limited slip system, presence of a second phase [5,6], and high temperature oxidation [7]. However, there have been few detailed studies on these issues of as-cast Ti-Ni-Hf alloys.

There have been numerous reports demonstrating that small additions (< 5%) of refractory elements can provide a uniform microstructure with a reduced grain size [8-10]. Kim *et al*. demonstrated that the addition of 0.30 wt% Sc to Al-Zn-Mg cast alloys resulted in significant grain refinements with fully equiaxed microstructure [11]. Furthermore, the improvement in the shape memory response of Ti-50.5Ni-24.5Pd alloys with Sc was reported by Atli *et al*. [12]. Regarding the Y effect, Liu *et al*. investigated the grain refining mechanism caused by Y in the primary a-Al in a semi-solid Al-7Si-0.3Mg alloy [13]. Semenova *et al*. investigated the phase equilibriums in the Ti-Ni-Y system at the TiNi-YNi section [14]. They noted that the solubility of Y in TiNi was approximately 0.3 at%. From an analogous perspective, it is expected that a small addition of Y could improve the high temperature properties of Ti-Ni-Hf alloys, as in other alloy systems. However, systematic investigations of the effects of Y in Ti-Ni-Hf have not yet been published.

The present study was undertaken in order to clarify the role of the Y addition in Ti-Ni-Hf alloys. A method of improving the hot workability and oxidation resistance without lowering the phase transformation temperatures was also sought. In order to achieve this, seven different program alloys with the same base chemical composition but different Y contents were produced in order to investigate the effect of Y on the thermal and mechanical properties.

2. EXPERIMENTAL PROCEDURES

2.1. Material preparation

Seven Ti-49Ni-10Hf alloys with different Y contents (0, 0.03, 0.3, 1, 2, 4.5, and 5.5 at%) were cast into button ingots

*Corresponding author: jh.kim@hanbat.ac.kr, yjt96@kims.re.kr

that were approximately 15 mm thick with a 40 mm diameter using a non-consumable vacuum arc melting method with a water-cooled copper crucible. Each alloy was melted at least three times in order to obtain sufficient mixing of the alloy ingredients. Then, the specimens were homogenized at 1000 °C for 24 h in order to avoid segregation of the alloying elements. Specimens of 4 × 8 × 20 mm for thermo-gravimetric analyses (TGA) were carefully cut from the master ingot and then ground on SiC papers up to 2000 grit in order to provide a smooth surface. Next, the specimens were ultrasonically cleaned in ethanol and dried before the oxidation tests. In order to investigate the microstructural evolution, a JSM-5800 microscope equipped with an energy dispersive spectroscope (EDS) was used for the scanning electron microscopy (SEM) observations.

2.2. Experimental procedures

Hot compression samples with a height of 12 mm and a diameter of 8 mm were sectioned in parallel to or perpendicular to the casting direction. The hot compression tests were conducted using a Gleeble 3500 system under vacuum conditions below 10^{-2} torr. The phase transformation behavior of the specimens was examined using differential scanning calorimetry (DSC) with a heating and cooling rate of 10 K/min. The measurements were performed in a helium atmosphere.

The oxidation experiments were performed using a SETARAM SETSYS evolution thermo-gravimetric analyzer (TGA). In order to ascertain the starting temperature of the oxidation of the Ti-Ni-Hf alloy, a heating oxidation test was conducted from room temperature to 1000 °C at a 5 °C min^{-1} heating rate in dry air. It has been previously confirmed that noticeable oxidation behavior begins above 700 °C [15]. Next, an isothermal oxidation test was conducted. First, the specimen was heated to the test temperatures of 900 and 1000 °C at a rate of 30 °C min^{-1} in a protective Ar gas. When the temperature reached the test temperature, the samples were oxidized in dry air, flowing at 16 ml min^{-1} for 100 h. The weight change of the specimen was measured as a function of the exposure time using the electronic balance technique in the thermo-gravimetric analyzer with an accuracy of 0.01 mg. After the test, the oxidized specimen was cooled to room temperature.

3. RESULTS

3.1. Microstructural evolution with Y addition

Figure 1 depicts the microstructures of the Ti-49Ni-10Hf alloys with Y content ranging from 0 to 4.5 at%. Figure 1(a) is the microstructure of the Ti-49Ni-10Hf base alloy, which contains elongated dark particles with lower amounts of Ni and Hf than the matrix (see Table 1). These dark particles were determined to be $(Ti+Hf)_2Ni$ particles, and their measured hardness levels were significantly higher than that of the matrix [7]. For the Ti-49Ni-10Hf-1Y alloy, white particles that preferentially precipitated along the $(Ti+Hf)_2Ni$ particles were observed (Fig. 1b). The Y content of these white particles (positions ③ and ④) was very high (< 67 at%), while the Ti and Hf contents were relatively low.

The atomic ratio between Ni and Y in the Y rich particles

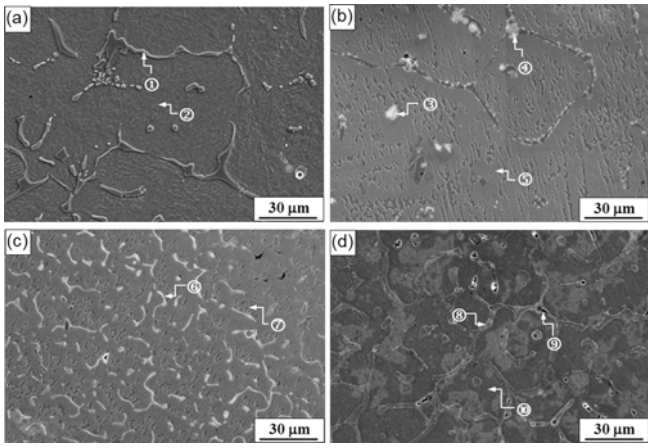

Fig. 1. SEM photos showing the microstructures of (a) Ti-49Ni-10Hf, (b) Ti-49Ni-10Hf-1Y, (c) Ti-49Ni-10Hf-2Y, and (d) Ti-49Ni-10Hf-4.5Y alloys.

Table 1. Chemical composition analysis of the microstructures in Fig. 1

Alloys	EDS position	Composition (at %)			
		Ti	Ni	Hf	Y
Ti-49Ni-10Hf	①	65.7	27.1	7.2	0
	②	46.6	43.0	10.3	0
Ti-49Ni-10Hf-1Y	③	9.7	22.2	1.4	66.7
	④	13.1	37.2	3.2	46.5
	⑤	46.9	42.8	9.8	0.41
Ti-49Ni-10Hf-2Y	⑥	12.9	36.9	3.0	47.3
	⑦	46.9	42.4	10.2	0.51
Ti-49Ni-10Hf-4.5Y	⑧	2.1	25.7	0.8	71.3
	⑨	33.0	24.0	6.5	36.7
	⑩	44.3	42.2	11.2	0.52

varied from 2:3 to 1:3. This implied that the white particles might have a Ni-Y system. However, the Y content in the matrix phase (position ⑤) was very low below 0.5 at%. When the Y content increased to 2 at%, the volume fraction of white particles increased significantly while that of the $(Ti+Hf)_2Ni$ particles decreased (Fig. 1c). For Ti-49Ni-10hf-4.5Y, the color of the Y-rich particles changed from white to gray. These primarily consisted of Ni and Y, and the amount of Ti and Hf in the Y-rich particles was almost negligible (position ⑧). In contrast, some dark particles (position ⑨) contained significant amounts of Ti and Hf, as well as Ni and Y. The Ni/Y atomic ratio of the gray particles was close to 1:3, while that of the dark particles was 2:3. It should be noted that the Y content in the matrix phase was approximately 0.5 at% regardless of the overall Y addition. This finding is analogous to a previous report that the solubility of Y in Ti-Ni was not more than 0.3 at% [14].

3.2. High temperature compression tests

Figure 2 presents the flow stress-versus-strain curves obtained from the hot compression tests using the programmed alloys. The tests were conducted at 700 °C using the true strain rate of $10^{-2}s^{-1}$. There was a distinct difference in the flow curves with regard to the Y content. The Ti-49Ni-10Hf alloy without Y exhibited a steady-state flow behavior up to a strain of 1.2 after reaching a strain of 0.4. The appearance of a peak in the flow curve followed by the steady-state flow resulted from the dynamic recrystallization, which has already been observed by Belbasi *et al*. [5]. For the Y-added alloys, however, this steady-state flow behavior was not observed. Instead, a gradual flow softening occurred for the Ti-49Ni-10Hf-0.03Y and Ti-49Ni-10Hf-0.3Y alloys. In contrast, when the amount of Y addition was more than 1.0 at%, severe fractures or surface cracking at a relatively early stage of straining was seen. In particular, the total compressive strains to fracture were very low: less than 0.7 and 0.4 for Ti-49Ni-10Hf-2Y and Ti-49Ni-10Hf-4.5Y, respectively. For Ti-49Ni-10Hf-1Y, the total compressive strain was comparable with that of Ti-49Ni-10Hf. However, surface cracking occurred on the specimen during the test. This indicated that a Y presence in excess of 1.0 at% significantly deteriorated the hot workability of the Ti-Ni-Hf alloys. This harmful effect on the hot workability might result from the presence of Y-rich particles along the grain boundaries.

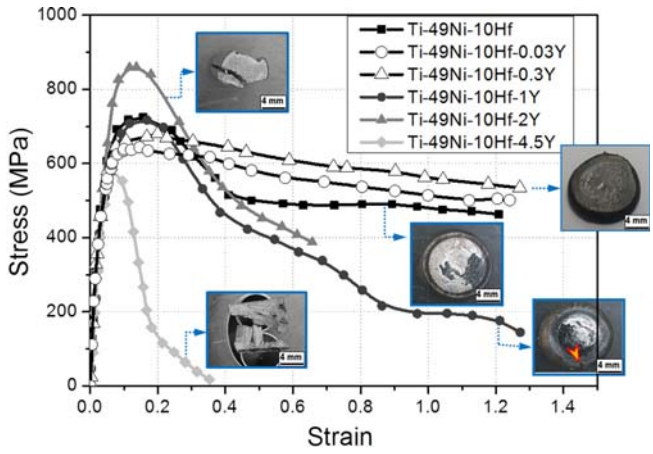

Fig. 2. Compressive stress-versus-strain curves of Ti-49Ni-10Hf alloys with various Y contents. Compression tests were performed at 700 °C using the true strain rate of $10^{-2}s^{-1}$. The red arrow in the inset indicates the surface cracking location.

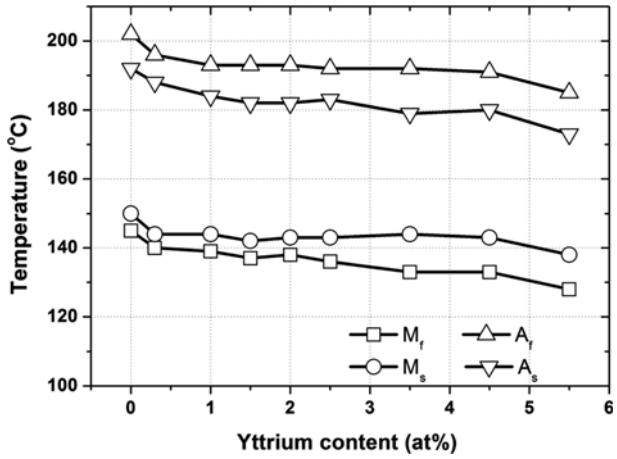

Fig. 3. Phase transformation temperatures as a function of Y content in Ti-49Ni-10Hf high temperature shape memory alloy (martensite finish, M_f; martensite start, M_s; austenite start, A_s; and austenite finish, A_f).

3.3. Effect of Y on phase transformation temperatures

Figure 3 presents the DSC results for the programmed alloys. The addition of Y at 1.0 at% decreased the transformation temperatures by approximately 10 °C. However, further additions of Y up to 4.5 at% did not result in a noticeable change in the martensite-austenite transformation temperatures, although

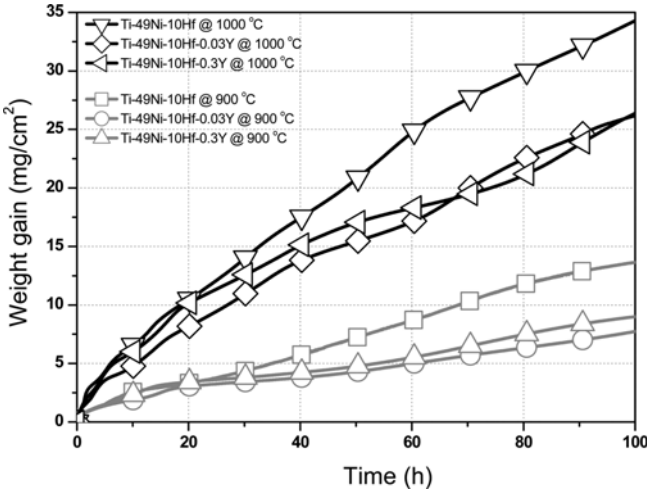

Fig. 4. Thermogravimetric curves of isothermal oxidation of Ti-49Ni-10Hf alloys with the Y content of 0, 0.03, and 0.3 at%, respectively. Tests were conducted at 900 and 1000 °C.

the martensite finish temperature decreased slightly. After the Y content was increased from 4.5 to 5.5 at%, a noticeable transformation temperature drop occurred, but it was not significant. This finding indicates that Y is not a strong high temperature phase stabilizer, unlike Sc, which is in the same group in the periodic table [16]. However, considering the fact that phase transformation temperatures can drastically change with a very small variation of Ni content [3], this finding is somewhat interesting because the precipitation of Ni-Y phase reduces the Ni content in the Ti-Ni-Hf matrix as shown in Table 1.

3.4. Effect of Y on high temperature oxidation

Figure 4 presents the weight gain-versus-time curves of the Ti-49Ni-10Hf alloys with 0, 0.03, and 0.3 at% Y. Oxidation tests were performed at 900 and 1000 °C for 100 h. According to the results depicted in the graph, the oxidation rate increased with the temperature for all test results. At 1000 °C, the oxidation kinetics was very fast from the initial starting condition compared with that at 900 °C. Sudden changes in slopes, which imply surface cracks or spallation in the oxide scale, were not observed in all test conditions.

It is noted that the overall oxidation rate was sufficiently reduced by a very small amount of Y addition at both temperatures of 900 and 1000 °C. The difference in the weight gain between the Ti-Ni-Hf alloy with and without Y became more distinct as the oxidation time increased. However, there was not a significant difference in the weight gain between the Y added alloys. The amount of weight gain of Ti-49Ni-10Hf-0.03Y was similar to that of Ti-49Ni-10Hf-0.3Y. This indicates that 0.03 at% Y is sufficient to enhance the high temperature oxidation resistance of Ti-Ni-Hf alloys.

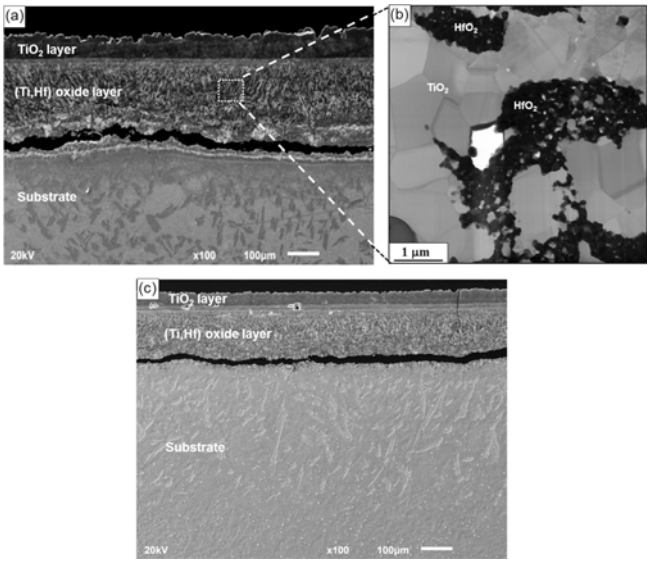

Fig. 5. Cross-sectional views of Ti-49Ni-10Hf and Ti-49Ni-10Hf-0.3Y alloys oxidized at 1000 °C for 100 hours; (a) SEM and (b) bright field TEM images of Ti-49Ni-10Hf, and (c) SEM image of Ti-49Ni-10Hf-0.3Y.

Figure 5a presents the cross-sectional morphologies of the Ti-49Ni-10Hf alloy after oxidation at 1000 °C for 100 h. Unlike most Ti alloys, the outermost TiO_2 layer was relatively thin at approximately 50 μm. In contrast, the thickness of the second layer, which is designated as the (Ti, Hf) oxide layer, was more than 200 μm and this oxide layer had the needle-like acicular structure of HfO_2. The TEM image revealed the detailed structure of this layer (see Fig. 5b). The needle-like acicular structure was an aggregate of HfO_2 nanoparticles, which were surrounded by the TiO_2 phase. It has already been reported that diffusion of Ti into a HfO_2 layer is very difficult [17,18]. Therefore, the formation of the TiO_2 layer on the top surface occurs very slowly because the diffusion of Ti in the matrix toward the surface is very sluggish. In contrast, the oxygen diffusion through HfO_2 is rapid; thus, oxygen can combine with Hf at the interface between the (Ti, Hf) layer and the matrix, and then HfO_2 forms [15].

The cross-sectional morphologies of the Ti-49Ni-10Hf-0.3Y and Ti-49Ni-10Hf-0.03Y alloys were also investigated. However, compared with Ti-49Ni-10Hf, there was no substantial difference in the microstructural observations (see Fig. 5c). This is ascribed to the amount of Y addition being very small compared with the other chemical elements. However, the total thickness of the oxide layers was substantially thinner in the Y-added specimen. In particular, the thickness of (Ti,Hf) oxide layer was reduced to ~120 μm with the addition of 0.3 at% Y.

4. DISCUSSION

Figure 1 demonstrates that Ti-49Ni-10Hf alloys with Y addition contained white particles of which the significant chemical elements were Ni and Y. Because the solubility of Y in Ti-Ni-Hf is below 0.5 at%, most Y exists in the form of a Ni-Y phase. In the present work, the Ni/Y atomic ratio in the Y rich particles was close to 1:3 or 2:3. This indicates that the white particles could be NiY_3 or Ni_2Y_3 phases. To date, limited research has been published on the ternary phase diagram of Ti-Ni-Y: the only available phase diagram has been provided by Zhuang [19] who constructed a 500 °C isothermal Ti-Ni-Y phase diagram. Assuming that there was not a significant difference between the room temperature and 500 °C phase equilibriums, the present findings are consistent with the results from the ternary phase diagram, which depicted the presence of NiY_3 or Ni_2Y_3 under similar chemical composition conditions. It has been reported that TiNi-NiY is a eutectic system with a wide range of two-phase alloys (TiNi + NiY) [14]. Considering the microstructural similarity between the Ti-Ni-Hf and Ti-Ni systems, the Ti-Ni-Hf based martensite/austenite phase should be surrounded by the eutectic YNi phase, as in the Ti-Ni system [16]. Because the Y content in the Ti-Ni-Hf matrix was below 1.0 at%, the chemical com-

positional effects on the phase transformation between the martensite/austenite phases should be very low. This explains the observation of small phase transformation temperature changes with Y content changes.

Figure 3 illustrates that the Y addition did not significantly lower the high temperature transformation properties of the Ti-Ni-Hf shape memory alloys. However, when the Y addition exceeded 1.0 at%, the high temperature ductility deteriorated. In contrast, the Y addition significantly enhanced the high temperature oxidation resistance at 900 and 1000 °C. Only a small amount of Y addition, i.e. < 0.03 at%, was sufficient for enhanced oxidation resistance and further improvements were not found with a 0.3 at% addition. Considering that the hot working and repeated annealing processes at 800-1000 °C are inevitable in this type of high temperature shape memory material, this beneficial effect is critical in terms of fabrication process flexibility [20]. Therefore, it is concluded that a Y addition of approximately 0.03 at% is necessary in order to improve the high temperature properties of Ti-Ni-Hf shape memory alloys. However, above 1.0 at% of Y, NiY_3 or Ni_2Y_3 particles formed along $(Ti,Hf)_2Ni$. These particles are expected to significantly promote crack initiation and propagation. Thus, Y addition above 1.0 at% should be avoided.

5. CONCLUSION

(1) Y addition to Ti-49Ni-10Hf alloys induced the precipitation of NiY_3 and Ni_2Y_3 phases preferentially along the $(Ti,Hf)_2Ni$ particles.

(2) The martensite-austenite transformation temperatures were not significantly influenced by Y additions of < 4.5 at%.

(3) Y additions above 1.0 at% deteriorate the hot workability of Ti-49Ni-10Hf. However, in contrast, a small amount of Y addition below 0.3 at% can effectively improve the high temperature oxidation resistance without loss of high temperature workability.

REFERENCES

1. G. S. Firstov, J. Van Humbeeck, and Y. N. Koval, *Scr. Mater.* **50**, 243 (2004).
2. G. S. Firstov, J. Van Humbeeck, and Y. N. Koval, *Mater. Sci. Eng. A* **378**, 2 (2004).
3. S.-W. Choi, H.-S. Lee, Y.-M. Jeon, T.-H. Nam, J.-T. Yeom, S.-W. Kim, C.-H. Park, J.-K. Hong, C.-S. Oh, and J. H. Kim, *Korean J. Met. Mater.* **53**, 151 (2015).
4. C. C. Wojcik, *J. Mater. Eng. Perf.* **18**, 511 (2009).
5. M. Belbasi, M. T. Salehi, S. A. A. A. Mousavi, and S. M. Ebrahimi, *Mater. Sci. Eng. A* **560**, 96 (2013).
6. P. E. Thoma and J. J. Boehm, *Mater. Sci. Eng. A* **273-275**, 385 (1999).
7. J. H. Kim, C. H. Park, S. W. Kim, J. K. Hong, C.-S. Oh, Y. M. Jeon, K. M. Kim, and J. T. Yeom, *J. Nano. Nanotech.* **14**, 9548 (2014).
8. M. J. Jones and F. J. Humphreys, *Acta Mater.* **51**, 2149 (2003).
9. J. H. Kim, K. M. Kim, T. S. Byun, D. W. Lee, and C. H. Park, *Thermochim. Acta* **579**, 1 (2014).
10. P. Żywicki, T. Abe, H. Garbacz, Y. Yamabe-Mitarai, and K. J. Kurzydłowski, *Met. Mater. Int.* **21**, 617 (2015).
11. J. H. Kim, J. T. Yeom, J. K. Hong, S. Y. Shim, S. G. Lim, and N. K. Park, *Met. Mater. Int.* **16**, 669 (2010).
12. K. C. Atli, I. Karaman, R. D. Noebe, A. Garg, Y. I. Chumlyakov, and I. V. Kireeva, *Metall. Mater. Trans.* **41A**, 2485 (2010).
13. Z. Liu, Y. Hu, and X. Liu, *Acta Metall. Sin.* **23**, 277 (2010).
14. O. Semenova, T. Khomko, and V. Petyukh, *Powder Metall. Met. C+* **46**, 274 (2007).
15. K. M. Kim, J. T. Yeom, H.-S. Lee, S.-Y. Yoon, and J. H. Kim, *Thermochim. Acta* **583**, 1 (2014).
16. Y. V. Kudryavtsev and E. Semenova, *Powder Metall. Met. C+* **48**, 700 (2009).
17. Z. X. Jiang, K. Kim, J. Lerma, D. Sieloff, H. Tseng, R. I. Hegde, T. Y. Luo, J. Y. Yang, D. H. Triyoso, and P. J. Tobin, *Appl. Surf. Sci.* **252**, 7172 (2006).
18. M. Xueli, H. Kai, and W. Wenwu, *J. Semicond.* **34**, 7 (2013).
19. Y. Zhuang, Y. Luo, and W. He, *J. Alloy. Compd.* **298**, 135 (2000).
20. Y. I. Son, C. H. Chung, R. R. Gowkanapalli, C. H. Moon, and J. S. Park, *Met. Mater. Int.* **21**, 1 (2015).